PHYSICAL REVIEW B VOLUME 27, NUMBER 2 15 JANUARY 1983

Electronic structure of metal hydrides. VI. Photoemission studies and band theory of VH, NbH, and TaH

D. J. Peterman*
Synchrotron Radiation Center, University of Wisconsin—Madison, Stoughton, Wisconsin 53589

D. K. Misemer
Ames Laboratory and Department of Physics, Iowa State University, Ames, Iowa 50011

J. H. Weaver
Synchrotron Radiation Center, University of Wisconsin—Madison, Stoughton, Wisconsin 53589

D. T. Peterson
Ames Laboratory and Department of Materials Science and Engineering, Iowa State University, Ames, Iowa 50011

(Received 14 June 1982)

The electronic structures of VH_x, NbH_x, and TaH_x ($0.6 \leq x \leq 1.0$) have been studied with the use of photoemission spectroscopy with synchrotron radiation ($10 \leq h\nu \leq 100$ eV). Two hydrogen-derived features are observed at ~ 5.5- and 7.5-eV binding energies, and the metal d bands are shown to be modified by the hydrogen interaction. These results show no agreement with rigid-band models based on the density of states of the pure metals and relatively poor agreement with previous band-structure calculations for monohydrides. We have calculated the energy bands of γ-phase NbH (self-consistently) and of NbH_0 and NbH_2 (non-self-consistently). Together, the calculations and experiments show how the metal-hydrogen interaction alters the electronic properties of the bcc metals.

I. INTRODUCTION

Understanding the role of hydrogen in metals is a matter of much scientific interest as well as technological importance.[1–3] Many hydrides drastically differ from their parent metals in terms of crystal structure, electronic structure, and mechanical properties. For some metals, these changes lead to valuable hydrogen storage capabilities, while for others, even small concentrations of hydrogen lead to serious embrittlement problems.

One of the most fundamental approaches to understanding the influence of hydrogen in metals involves a systematic study of the electronic structure of metal hydrides. A great deal of theoretical groundwork in the form of energy-band calculations has been provided by Switendick.[4] Our own recent work[5–9] has combined optical and photoemission spectroscopies with band-structure calculations to obtain a detailed understanding of the electronic structure of metal hydrides. To date, we have focused largely on the group-III*B*, -IV*B*, and rare-earth di- and tri-hydrides. We now present a study of the group-V*B* transition-metal mono- and submono-hydrides.[10]

The group-V*B* metal hydrides exist with several ordered and disordered hydrogen phases. An excellent review of these structures may be found in Ref. 11. The metal lattice is bcc or a slight distortion thereof and the hydrogen atoms occupy the tetrahedral sites in most phases. Within the context of band theory, these hydrides are difficult systems to work with because of their complicated crystal structures and low symmetry. In order to make the band calculations more tractable, more symmetric lattices are often chosen as a first approximation. Experimentally, these hydrides are also difficult to work with because, without cooling, there is hydrogen diffusion through the vacuum-surface interface after the polycrystalline samples are fractured to perform the ultrahigh-vacuum photoemission measurements. Despite these difficulties, the group-V near-monohydrides offer valuable opportunities for understanding the interaction of hydrogen with metals.

Using photoemission spectroscopy, we have examined the electronic structure of polycrystalline VH_x, NbH_x, and TaH_x ($0.6 \leq x \leq 1.0$), NbD_x ($0.6 \leq x \leq 0.8$), and single-crystal Nb_4D_3. Of particular interest to us was the extent to which the rigid-band approximation (RBA) could be applied to the metal to understand these hydrides. On the one hand,

specific-heat and magnetic susceptibility experiments have suggested that a band filling is taking place so that near E_F the RBA is quite good.[12] On the other hand, the band calculations by Switendick[4,13] for VH and by Gupta and Burger[14] for NbH show a low-lying, splitoff band not predicted by the RBA. Experimental evidence for such hydrogen-induced states has been seen with x-ray spectroscopy.[15,16] While our measurements clearly showed the presence of low-energy features and the limitations of the RBA, they did not agree well with the previous calculations, and we were led to perform our own calculations using a more realistic crystal structure.

Using the self-consistent (SC) Korringa-Kohn-Rostoker (KKR) method, we have performed energy-band calculations of γ-phase (pseudocubic) NbH. In addition, we have calculated non-self-consistent (NSC) energy bands for γ-NbH_0 (same lattice structure as γ-NbH but with no hydrogen) and δ-phase NbH_2 (CaF_2 structure). These calculations provide a theoretical picture of the hydrogen-induced changes in the electronic structure of the metal and provide the perspective necessary to understand the photoemission results.

In the following, we discuss our experimental and theoretical studies of the electronic structure of the group-V*B* metal hydrides, emphasizing the changes which occur upon hydride formation. In Sec. II we present the experimental details and results of our photoemission measurements and compare them to the previous band-structure calculations.[4,14] In Sec. III we present our own calculations, and compare them to the previous calculations and to our photoemission results. In Sec. IV we summarize our findings, discussing differences between the various calculations and between experiment and theory.

II. EXPERIMENTAL DETAILS AND RESULTS

Most of the samples used in this study were prepared in bulk form starting with high-purity V, Nb, or Ta from the Ames Laboratory. The metals typically contained less than 500 atomic parts per million (ppm) total metallic impurities and less than 200, 100, and 200 at. ppm of O, N, and C, respectively. The samples were charged with hydrogen, as described previously,[9] by first heating them under vacuum at temperatures of $\simeq$1000 °C and then holding them at a controlled hydrogen pressure with a temperature appropriate to obtain the desired concentration. Several samples of NbD_x, $0.6<x<0.8$, were also prepared in a similar fashion. The samples were analyzed for hydrogen content by using a hot-vacuum extraction technique with an estimated accuracy of $\sim$2%. In addition to the polycrystalline samples, we examined a single crystal of Nb_4D_3. Since all samples were to be fractured in the vacuum of the photoemission chamber, no surface preparation was required.

The photoemission experiments were carried out at the Synchrotron Radiation Center of the University of Wisconsin using radiation emitted by 240-MeV electrons in the storage ring Tantalus. The light was dispersed by either a 3-m toroidal grating monochromator (photon energy range of $10<h\nu<100$ eV) or by a Seya-Namioka monochromator ($10<h\nu<30$ eV). The base pressure of the system was typically $\lesssim\times10^{-11}$ torr prior to fracturing. For the hydrides, a closed-cycle helium refrigerator was used to cool the samples to $\sim$50 K to prevent the loss of hydrogen after fracturing the samples. Upon fracturing there was a hydrogen burst, bringing the pressure up to as high as 10^{-9} torr, after which the system slowly recovered ($\sim$1 h) to $<1\times10^{-10}$ torr. It is unknown how much of the pressure increase was due to sample fragments which warmed up after not being caught in the cold collection basket during the fracturing process. The niobium deuteride samples required no cooling, and no deuterium loss upon fracturing was observed by

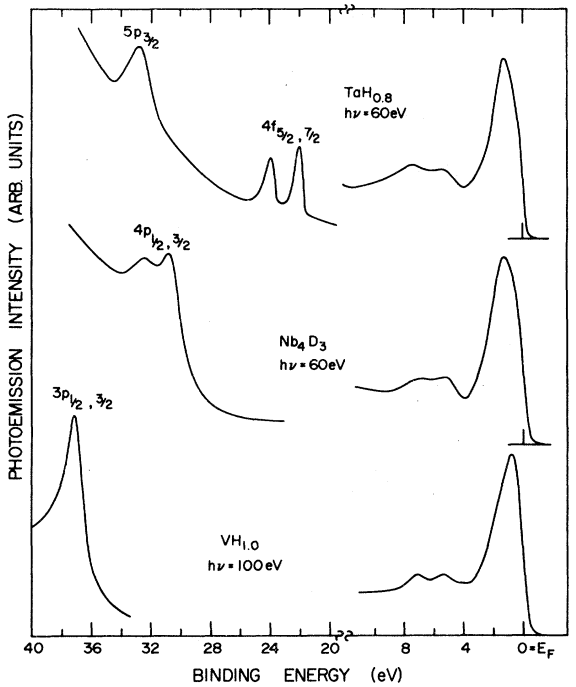

FIG. 1. Photoelectron energy distribution curves (EDC's) for VH, Nb_4D_3, and $TaH_{0.8}$. The binding energies of the V, Nb, and Ta $p_{3/2}$ core levels are 37.1, 30.7, and 32.7 eV, respectively. As discussed in the text, the features between 4 and 9 eV are hydrogen induced.

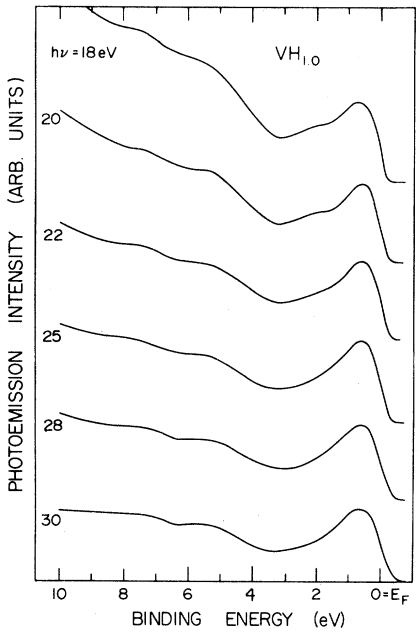

FIG. 2. Photoelectron EDC's of VH for $18 \leq h\nu \leq 30$ eV. The two high-binding-energy features near 5.5 and 7.5 eV are nearly invisible at these energies; for $h\nu \lesssim 20$ eV a shoulder emerges in the d bands ~ 2.0 eV below E_F.

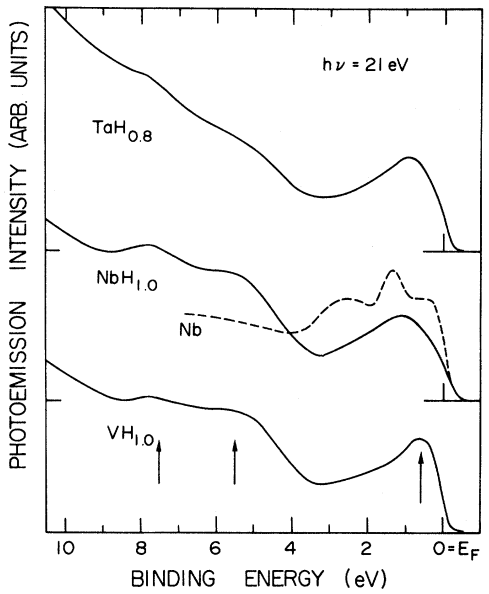

FIG. 3. Photoelectron EDC's of $VH_{1.0}$, $NbH_{1.0}$, and $TaH_{0.8}$ showing the similarities in the spectral features. Comparison to the dashed line, which is an EDC of Nb at $h\nu = 21.2$ eV (angle-integrated photoemission, recrystallized {110} foil, Ref. 20), highlights the changes in electronic structure due to the presence of hydrogen. The two features at high binding energy are seen to be hydrogen derived and the d bands appear narrower and show less structure.

the quadrupole residual gas analyzer. Comparison of the deuteride and hydride spectra evidenced no significant difference. After fracturing, the samples were translated immediately to the common focus of the light and the double-pass cylindrical mirror analyzer. The experimental geometry has been described in detail elsewhere.[17] In addition, the general use of photoelectron spectroscopy for studies of hydrides has been discussed in paper III of this series.[7]

Representative photoelectron energy distribution curves (EDC's) for $VH_{1.0}$, $NbH_{1.0}$, Nb_4D_3, and $TaH_{0.8}$ are shown in Figs. 1–3. In Fig. 1 an overview is provided which includes the respective p and f core levels. The binding energies of the $p_{3/2}$ core levels are 37.1, 30.7, and 32.7 eV for the hydrides (deuterides) of V, Nb, and Ta, respectively, while the Ta $4f_{7/2}$ has a binding energy of 22.1 eV. These values may be compared to reported values for the bulk elemental metals which are, respectively, 37.1, 30.8, and 32.7 eV for the $p_{3/2}$ levels[18] and 21.6 eV for the Ta $4f_{7/2}$.[18,19] No clear evidence of charge transfer is obtained by comparing these results and, as we shall see, this agrees with the band calculations. In Fig. 2 the $h\nu$ dependence of $VH_{1.0}$ is shown for $18 \leq h\nu \leq 30$ eV—the behavior of the other hydrides and deuterides was quite similar. These spectra have been normalized to a constant height of the feature near E_F. Figure 3 displays EDC's obtained using a photon energy of 21 eV. Earlier photoemission studies with dihydrides showed that this was a favorable photon energy for comparing experiment to theory via a calculated density of states (DOS).[9] Three features are highlighted by arrows in Fig. 3. We found that with different fractures the magnitude of the two weakly emitting features near 5.5 and 7.5 eV binding energy varied with respect to that of the first feature near E_F, but they always had the same magnitude relative to each other. The shape and width of the feature near E_F were very reproducible.

The comparison of NbH to Nb (Ref. 20) in Fig. 3 provides an experimental picture of the effect of hydrogen on the electronic structure of niobium. The most obvious difference is the appearance of two new hydrogen-derived features at binding energies of $\simeq 5.7$ and 7.4 eV. These, of course, would not be predicted by the RBA. Another important metal-to-hydride change is that structure in the metal bands has been lost, with the Nb states farthest below E_F being drawn and hybridized with the hydrogen; as we shall see in Sec. III, these states have the most s character. An important observation is that the width of the d-derived feature in the hydride (the structure closest to E_F) has decreased,

also in contradiction to the rigid-band model. We therefore turn to band theory for a more detailed understanding of the hydrogen-induced changes in the electronic structure of Nb.

Before doing so, however, the reader should note that the results reported here are for polycrystalline samples of NbH and that the comparison to Smith's results must be made with caution. First, Smith was dealing with recrystallized foils of Nb(110). Second, although we both used double-pass cylindrical mirror electron-energy analyzers, the $\vec{k}$-space averaging would be geometry dependent, even if we had had single crystals. Third, our hydride exhibits a distorted bcc crystal structure and the details of the electronic structure would vary slightly. Nevertheless, the major points to be made remain that the hydride exhibits new H-induced electronic features below the d bands and that the apparent width of the d band is considerably reduced compared to Nb metal.

In Fig. 4 energy-band calculations of VH and NbH are compared to the background-subtracted photoemission spectra from Fig. 3. At the top, the VH DOS calculated by Switendick[4,13] shows several hydrogen-derived features with a center located at

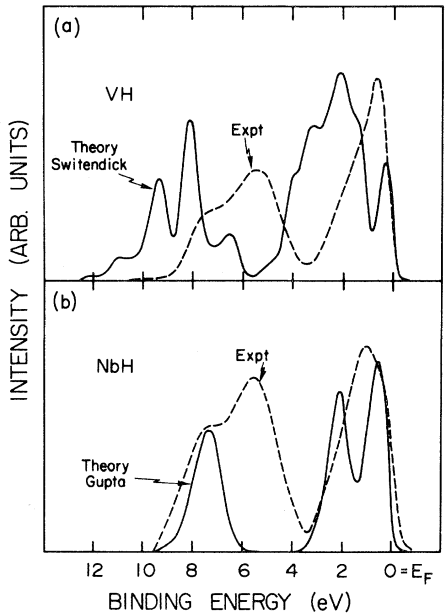

FIG. 4. Background-subtracted EDC's (dashed lines) from Fig. 3 compared to theoretical density of states (DOS) calculations for VH from Ref. 4 and NbH from Ref. 14. The calculated DOS's have been Gaussian broadened and cut off at E_F for comparison to experiment. As discussed in the text, the rather poor agreement can be related in part to the overly simplified crystal structures. The crystal structures used for these calculations are shown in Fig. 5.

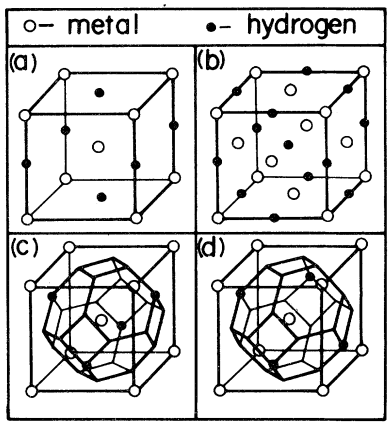

FIG. 5. Crystal structures considered for the various energy-band calculations. (a) The bcc metal lattice with hydrogen in octahedral sites used in Switendick's calculations (Refs. 4 and 13) [see Fig. 4(a)]. (b) The fcc metal lattice with H in octahedral sites used in Gupta's calculations (Ref. 14) [see Fig. 4(b)]. (c) The pseudocubic γ phase of NbH used in the present calculation. (d) The β-phase of NbH with H in different tetrahedral sites than those in (c).

$\sim$2 eV higher binding energy than indicated by experiment. Most disturbing is the disagreement with the width of the remaining, primarily metal-derived states near E_F [experimental full width at half maximum (FWHM) $\sim$2 eV, theoretical FWHM $\sim$4 eV]. One possible reason for this discrepancy is that the crystal structure used for the calculation was unrealistic: bcc metal lattice with hydrogen in the octahedral sites at $(0,0,a/2)$ above each metal atom as shown in Fig. 5(a).

Gupta and Burger[14] assumed a different crystal structure for NbH [fcc metal lattice with hydrogen occupying the octahedral sites, Fig. 5(b)] and their calculated DOS is compared with experiment in Fig. 4(b). This calculation shows only one hydrogen-derived feature split off from the metal states and displays a much narrower metal feature compared to the DOS calculated by Switendick for VH [Fig. 4(a)]. While the overall width of the metal states shows moderate agreement with experiment, the splitting of the d bands into two widely separated metal-derived peaks was not observed. Once again, we are led to question the influence of crystal structure on the calculations.

Examination of the various phase diagrams[11] for VH, NbH, and TaH shows that the metal retains a nearly bcc lattice and that the hydrogen atoms primarily occupy tetrahedral sites, not the octahedral sites used in earlier calculations. One particularly symmetric phase of NbH, the γ phase or pseudocubic phase, is shown in Fig. 5(c). Motivated by the poor agreement between experiment and existing

calculations, we carried out energy-band calculations using this γ-phase crystal structure.

III. CALCULATIONAL DETAILS AND RESULTS

First-principles electronic band-structure calculations using the KKR method were carried out for γ-phase NbH using the reported[11] lattice constant of 3.461 Å. Initial NSC calculations using full Slater exchange ($\alpha=1$) did not provide adequate agreement with experiment, so the calculations were brought to self-consistency using the local-density approximation (LDA) described by Hedin and Lundqvist.[21] In addition to this SC calculation, NSC calculations of NbH_0 (LDA using the γ-NbH lattice structure with a muffin-tin sphere at the unoccupied hydrogen site) and NbH_2 (Slater exchange using the CaF_2 structure) were performed. The NbH_2 calculation was also carried out, as will be discussed, for comparison to the photoemission experiments. Here, the reported[11] δ-phase (CaF_2-structure) lattice constant of 4.546 Å was employed. Except for the dihydride calculations, an atomic hydrogen charge density was overlapped with the d^4s^1 Nb charge density. For the δ phase, the d^3s^2 configuration was used, since it was found in our previous work with the group-III*B* metals that these NSC results most closely approximate the self-consistent results.[6] For the NbH_2 calculation, the wave functions were expanded through $l=3$ and 1 for the metal and hydrogen spheres, respectively, while for the remaining work the expansions were through $l=3$ and 2.

For NbH and NbH_0, eigenvalues were determined at 80 points in the irreducible $\frac{1}{16}$ of the Brillouin zone picked following the special point scheme of Chadi and Cohen.[22] For the SC calculation the eigenvalues and total charge within the muffin-tin spheres were converged to 1 mRy and 0.003 electrons, respectively. The sphere sizes were chosen, as before,[6] such that the metal sphere extended 65% of the way to the hydrogen site. Based upon the results of Papaconstantopoulos *et al.*[23] for PdH, we do not expect the *d*-like energy bands near E_F to be particularly sensitive to the relative sphere sizes. Additional details, especially concerning dihydride calculations with the CaF_2-type crystal structure, may be found elsewhere.[6]

The NbH_0 calculation provides an excellent perspective for understanding the H-induced changes in the electronic structure of γ-NbH. The energy bands for γ-NbH_0 and γ-NbH are shown in Fig. 6. The symmetries for the hydride are labeled for a bcc lattice but, due to the lower symmetry imposed by the location of the hydrogen atoms, the subscripts

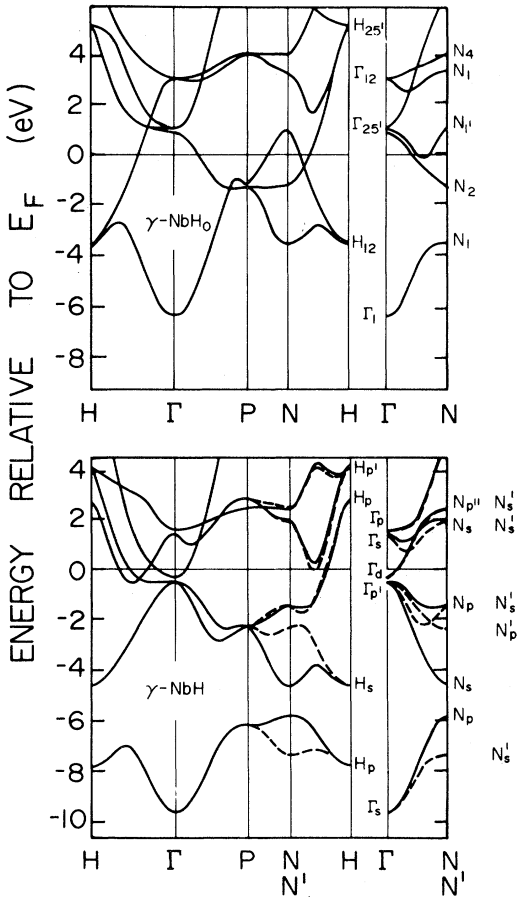

FIG. 6. Electronic energy bands of γ-NbH and γ-NbH_0 (γ-NbH lattice with empty muffin-tin spheres at the hydrogen sites). *N* and *N'* denote two inequivalent points given by $(\pi/2a,\pi/2a,0)$ and $(\pi/2a,0,\pi/2a)$, respectively. The symmetry assignments are discussed in the text.

have been chosen following Ref. 24. Compared to bcc Nb, the irreducible part of the Brillouin zone now comprises $\frac{1}{16}$ rather than $\frac{1}{48}$ of the total zone volume and two inequivalent *N* points are thus shown for the hydride. The lower symmetry in NbH_0 (lower because of the interstitial spheres) lifts some degeneracies that occur in cubic Nb (Ref. 25) but the energy eigenvalue differences are small and we give the standard cubic symmetry assignments. A comparison of the metal and hydride bands shows that the largest changes, besides the splitting off of the lower band, involve portions of the Brillouin zone near *N*. These changes are further highlighted in Fig. 7, where the partial densities of states of the metal and hydride are compared. The energy zero has been chosen to give a state occupation of six electrons in both NbH_0 and NbH. This choice allows an examination of the degree to which rigid-

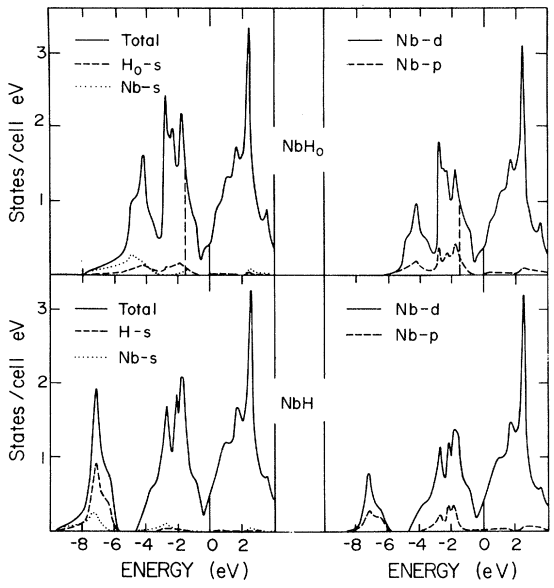

FIG. 7. Total and partial DOS for NbH_0 (upper) and NbH (lower). The H_0 denotes the empty muffin-tin sphere in the NbH_0 calculation. The energy scale is drawn relative to E_F for the hydride. For NbH_0, the dashed line denotes E_F, while the energy zero corresponds to the rigid-band addition of one electron to Nb.

band behavior is followed in going from the metal to the hydride (the dashed line in the top figure indicates the actual Nb Fermi level). As is apparent from the figure, it is the extended metal s states which are most affected by the presence of hydrogen. The primary effect of adding hydrogen to the lattice is a lowering and hybridization of metal states that were already occupied and were located at greater than 3 eV below E_F. Thus the Fermi level must rise to accommodate the extra electron. The high degree of similarity between the DOS of NbH and that of NbH_0 near E_F helps explain why the rigid-band picture has met with some success in discussing hydrogenation characteristics observed using various Fermi-surface-sensitive experiments.[12] Band theory, of course, goes beyond that simple model and reveals the rich detail of the hydrogen-induced changes.

The large change in the Fermi level should not be taken to mean that the electron is transferred to the metal. In fact, starting from the atomic charge densities, 0.17 electrons were transferred into the hydrogen sphere, while 0.46 electrons left the metal sphere (the difference is in the interstitial region). Table I details the charge transfer in the SC calculations and also compares the NSC metal and hydride charge densities. From the table, one can see that a significant amount of metal charge is included in the hydrogen spheres and thus screens the proton. The similarity of the charge in the metal spheres in both NSC calculations, coupled with the high degree of screening of the proton, leads one to expect no significant charge transfer from the metal. In going to self-consistency with γ-NbH, the charge goes toward the metal and away from the hydrogen site. However, a similar charge transfer is expected in the metal due to electron-electron repulsion in the interstitial region and to the attraction of the ion cores. This is corroborated by the p core-level measurements presented in Sec. II, since they also argue for a small amount of charge transfer.

In Fig. 8 we compare the results of the various calculations with background-subtracted experimental spectra. The calculated DOS in each case has been cut off at E_F and Gaussian broadened to facilitate the comparison. In Fig. 8(a) we show our NbH_0 calculation and the photoemission results of Smith[20] (a background has been subtracted from the EDC in Fig. 3). As shown, the agreement is quite good even though the lattice constant used in the calculation was that of γ-NbH and therefore 5% larger than that of Nb. Overall, the calculated features are within a few tenths of an electron volt of the corresponding experimental features. For NbH, however, the agreement between the γ-phase calculation and the experiment is not nearly as satisfactory [Fig. 8(b)]. The calculation predicts only one hydrogen-derived peak at -7.1 eV (FWHM ~ 1.1 eV), whereas two are found experimentally (FWHM ~ 3.9 eV). Furthermore, the discrepancy in the width of the occupied d states is very large and is similar to that which was found in the VH comparison of Fig. 4(a).

TABLE I. Charge contained in muffin-tin spheres for the NbH and NbH_0 calculation. Note (*) that there is a muffin-tin sphere at the hydrogen site in the NbH_0 calculations but that it contains no proton.

	Charge in muffin-tin spheres							
	Atomic		Superimposed atomic		NSC		SC	
Calculation	Nb	H*	Nb	H*	Nb	H*	Nb	H*
NbH	38.589	0.398	39.168	0.579	38.470	0.822	38.707	0.751
NbH_0	38.589	0	38.957	0.179	38.477	0.237		

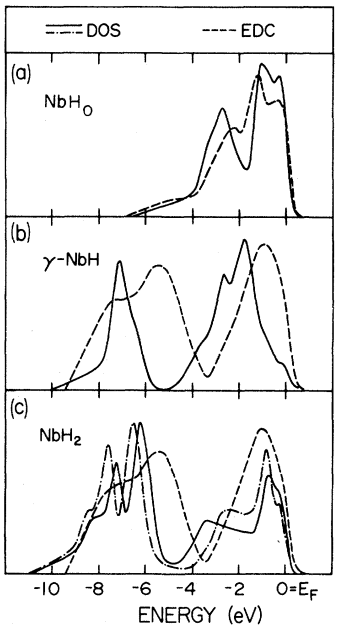

FIG. 8. Photoelectron EDC's compared to band calculations. In (a) the EDC of Smith (Ref. 20) is compared to our NbH_0 calculation. In (b) our NbH EDC of Fig. 3 is compared to our calculation of γ-phase NbH. In (c) the same NbH EDC is compared to our calculation of NbH_2 (solid line) and to that of Gupta (dot-dashed line, from Ref. 26).

In Fig. 8(c) we compare our NbH_2 calculation with similar work by Gupta[26] and with our experimental results for NbH_1. The augmented-plane-wave calculation by Gupta differs from ours due to her use of a warped muffin-tin potential and a d^4s^1 rather than a d^3s^2 metal configuration. Such warping becomes more important when, as in this crystal structure, a large portion of the Brillouin zone is outside the muffin-tin spheres (52% outside) which are centered on the atoms.[27] In comparison to experiment, better agreement is obtained with the NbH_2 than with the NbH calculations. Especially attractive in the NbH_2 DOS are the *two* hydrogen features and the narrower metal bands. It is clear from the spectra, however, that the hydride being studied is not in a pure surface δ phase. This conclusion is consistent with the work of Birnbaum *et al.*[28] and in the next section we discuss the implications of these experimental and theoretical results.

IV. SUMMARY AND CONCLUSIONS

In the previous two sections we have provided an experimental and theoretical picture of the affect that hydrogen has on the electronic structure of V, Nb, and Ta hydrides. Experimentally, we find that two hydrogen-induced features appear well below the metal d bands and, in comparison to similar measurements of Nb metal, the remaining d-like states show no evidence of rigid-band-like behavior. On the other hand, band theory for γ-NbH predicts only one hydrogen-induced feature and suggests that within 3 eV of E_F the RBA is not altogether unreasonable because the more localized d states near E_F are relatively unaffected by the metal-hydrogen interaction. Band theory, which shows excellent agreement with photoemission results for Nb [Fig. 8(a)], shows very poor agreement with photoemission results for NbH [Fig. 8(b)].

Since band theory has successfully described photoemission results for many other hydrides,[5–9] one would like to reconcile the apparent disagreement for the monohydrides. The calculational assumption that the experimentally sampled region is bulk γ-NbH-like must be questioned. The β phase may be a more reasonable assumption for the bulk crystal structure because it is a more prevalent high-concentration phase.[11] On the other hand, the surface of our samples may be different from the bulk. Recent measurements by Strongin and coworkers[29] of H uptake in Nb indicated a substantially higher surface hydrogen concentration than found in the bulk and they postulated that a surface hydride of unknown composition overlays the bulk solid solution. The creation of a modified surface region when the hydride is fractured is consistent with the embrittlement studies of Birnbaum *et al.*[28] With the use of the scanning electron microscopy, electron diffraction, ion probe, and crystallographic evidence, these workers found that a cleavage fracture occurred through a stress-induced β-phase hydride, even in samples containing only 2.1 at. % hydrogen. This would explain our experimental observation that the photoemission spectra are much less sensitive to the bulk H concentration than would be predicted based on changes expected from a rigid-band shift of the Fermi level of γ-NbH. If, within the escape depth of the photoelectron ($\sim$8–20 Å), the crystal is in an other-than-bulk γ-NbH configuration, substantial differences between the photoemission spectra and the calculated DOS are possible.

In Fig. 5(d) we show the crystal structure for the β phase of NbH. Aside from a small distortion of the cubic bcc metal lattice, the major difference between the β and γ phases is that different tetrahedral sites are occupied by hydrogen atoms. The question then is whether or not electronic interactions in the β phase would be sufficiently different from those in the γ phase that they would give rise to two splitoff hydrogen features and a less rigid-band-like shift of E_F (i.e., more agreement with photoemission). Without performing the cal-

culation one can only speculate but, because of the different coordinations and hydrogen-hydrogen distances, two H-induced features do seem likely. With two formula units per unit cell, the new symmetry raises the intriguing possibility of the formation of a hydrogen-hydrogen antibonding state, analogous to that in the dihydrides.[30] Furthermore, the H-H nearest-neighbor distance in β-NbH is 2.450 Å and is within the 2.2—2.8 Å range of the observed H-H separations in the stable dihydrides (in γ-NbH this distance is 3.010 Å). If, as in the dihydrides, more metal states are pulled down from above E_F to form such a dihydridelike band, it would allow E_F to lie closer to the energetically favorable d-band minimum. Thus, compared to γ-NbH, the occupied d-band width near E_F would be narrower, as is suggested by the photoemission experiments [Fig. 8(b)]. The details of the hydrogen-induced states, 4—8 eV below E_F, are even more sensitive to the position of the H atoms, as can be seen in Fig. 4. While the large bandwidth of the hydrogen-derived DOS in Switendick's calculation of VH can be attributed to the presence of two different metal-hydrogen distances (see Fig. 5), in β-NbH we expect an increased bandwidth due to the small H-H separation. The extreme sensitivity of *both* the hydrogen and metal features in the DOS to the H-H distance and symmetry location has been demonstrated through band calculations of YH_2 comparing the CaF_2 structure (2 tetrahedral sites occupied, H-H distance of 2.60 Å) to a modified structure (1 octahedral and 1 tetrahedral site occupied, H-H distance of 2.25 Å).[31] Hence, if there is a surface layer with structure significantly different from the γ-NbH phase, it is reasonable to expect the kind of disagreement observed here.

In order to resolve these issues, more theoretical and experimental input is necessary. Theoretically, a β-phase calculation would be invaluable. There is less symmetry but, with two formula units per unit cell, such a computation is certainly feasible. The value of a warped muffin-tin potential might also be explored since, in our γ-phase calculations, only 47% of the unit cell was within muffin-tin spheres. While, as Fig. 8(a) demonstrates, this is not a serious problem for Nb, the noncubic symmetry of the hydrogen may well lead to changes more severe than the CaF_2 case (which was also shown in Fig. 8). Experimentally, several investigations may be suggested. First, photoemission studies of cleaved α-phase NbH would reveal whether a surface hydride will form when low-concentration samples are fractured, and further studies of surface hydrogen chemisorbed on Nb would offer additional insight on the surface phase reported by Strongin *et al.*[29] Second, neutron scattering on similarly prepared samples should be performed to indicate the occupancy of nonideal sites. Such occupancy would guide the use of the calculated electronic structures in interpreting photoemission results.

ACKNOWLEDGMENTS

The authors wish to acknowledge the stimulating discussions with B. N. Harmon, D. R. Torgeson, and M. Strongin. H. Birnbaum generously provided the single crystal of Nb_4D_3. The technical support of A. D. Johnson and H. H. Baker in preparing the samples was invaluable, and the generous support of the staff of the Synchrotron Radiation Center is greatly appreciated. The work at the University of Wisconsin was supported by the U. S. Department of Energy under Contract No. DE-AC02-80ER-10584. The Ames Laboratory is operated for the U. S. Department of Energy by Iowa State University under Contract No. W-7405-Eng-82 and the work in Ames was supported by the Director for Energy Research, Office of Basic Energy Sciences. The Synchrotron Radiation Center is supported by the National Science Foundation under Grant DMR-80201644.

*Present address: McDonnell-Douglas Research Laboratories, McDonnell Douglas Corporation, St. Louis, Missouri 63166.

[1]W. M. Mueller, J. P. Blackledge, and G. G. Libowitz, *Metal Hydrides* (Academic, New York, 1968).

[2]D. L. Westlake, C. B. Satterthwaite, and J. H. Weaver, Phys. Today 31 (11), 32 (1978).

[3]J. J. Reilly and G. D. Sandrock, Sci. Am. 242, 118 (1980).

[4]A. C. Switendick, in *Hydrogen in Metals I: Basic Properties,* Vol. 28 of *Topics in Applied Physics,* edited by G. Alefeld and J. Völkl (Springer, New York 1978), Chap. 4.

[5]J. H. Weaver, R. Rosei, and D. T. Peterson, Phys. Rev. B 19, 4855 (1979), I of this series of studies.

[6]D. J. Peterman, B. N. Harmon, J. Marchiando, and J. H. Weaver, Phys. Rev. B 19, 4867 (1979), II of this series of studies.

[7]J. H. Weaver, D. T. Peterson, and R. L. Benbow, Phys. Rev. B 20, 5301 (1979), III of this series of studies.

[8]J. H. Weaver, D. J. Peterman, D. T. Peterson, and A. Franciosi, Phys. Rev. B 23, 1692 (1981), IV of this series of studies.

[9]D. J. Peterman, J. H. Weaver, and D. T. Peterson, Phys. Rev. B 23, 3903 (1981), V of this series.

[10]A preliminary report of these results was given at the

International Symposium on the Electronic Structure of Hydrogen in Metals, Richmond, Virginia, NATO series in Materials Science (Plenum, New York, in press).

[11]T. Schober and H. Wenzl, in *Hydrogen in Metals II: Application-Oriented Properties,* Vol. 29 of *Topics in Applied Physics,* edited by G. Alefeld and J. Völkl (Springer, New York, 1978), Chap. 2.

[12]E. Wicke, J. Less-Common Met. 75, 185 (1980), and references therein.

[13]A. C. Switendick, in *Hydrogen Energy, Part B,* edited by T. N. Veziroglu (Plenum, New York, 1975), p. 1029.

[14]M. Gupta and J. P. Burger, Phys. Rev. B 24, 7099 (1981).

[15]Y. Fukai, S. Kazama, K. Tanaka, and M. Matsumoto, Solid State Commun. 19, 507 (1976).

[16]I. A. Brytou, E. Z. Kurmaev, K. I. Konashenok, and M. M. Antonova, Izv. Akad. Nauk SSSR, Neorg. Mater. 9, 137 (1973) [Inorg. Mater. (USSR) 9, 137 (1973)].

[17]G. Margaritondo, J. H. Weaver, and N. G. Stoffel, J. Phys. E 12, 662 (1979); see also Ref. 7.

[18]J. C. Fuggle and N. Mårtensson, J. Electron Spectrosc. Relat. Phenom. 21, 275 (1980).

[19]J. F. van der Veen, F. J. Himpsel, P. Heimann, and D. E. Eastman, Solid State Commun. 37, 555 (1981).

[20]R. J. Smith, Phys. Rev. B 21, 3131 (1980).

[21]L. Hedin and B. I. Lundqvist, J. Phys. C 4, 2064 (1971).

[22]D. J. Chadi and M. L. Cohen, Phys. Rev. B 8, 5747 (1973).

[23]D. A. Papaconstantopoulos, B. M. Klein, E. C. Economou, and L. L. Boyer, Phys. Rev. B 17, 141 (1978).

[24]D. G. Bell, Rev. Mod. Phys. 26, 311 (1954).

[25]See, for example, K. M. Ho, S. G. Louie, J. R. Chelikowsky, and M. L. Cohen, Phys. Rev. B 15, 1755 (1977).

[26]M. Gupta, Phys. Rev. B 25, 1027 (1982).

[27]The need for a warping correction can be lessened by the inclusion of an empty muffin-tin sphere at the octahedral site. For the group-III*B* metal dihydrides, self-consistent results using this approach showed that for the *d*-band width, a NSC calculation without the empty sphere but using the metal s^2 configuration in charge overlap was quite reasonable. See also, D. J. Peterman and B. N. Harmon, Phys. Rev. B 20, 5313 (1979).

[28]M. L. Grossbeck and H. K. Birnbaum, Acta Metall. 25, 135 (1977); S. Gahr and H. K. Birnbaum, *ibid.* 26, 1781 (1978); only when the temperature is greater than $\sim$150 °C do they find that a surface dihydride is formed, otherwise the β-phase monohydride is formed at the fracture.

[29]M. Strongin, J. Colbert, G. J. Dienes, and D. O. Welch, Bull. Am. Phys. Soc. 27, 162 (1982).

[30]The formation of a hydrogen-hydrogen antibonding state in the monohydrides of Cr and Cu, where there are also two formula units per unit cell, is discussed in A. C. Switendick, Int. J. Quantum. Chem. 5, 459 (1971).

[31]D. J. Peterman, B. N. Harmon, D. L. Johnson, and J. Marchiando, Z. Phys. Chem. (Frankfurt am Main) Neue Folge 116, 491 (1979).